

Article

Analysis of the Self-Cleaning Potential of Glass Fiber Reinforced Concrete (GRC) with TiO₂ Nanoparticles

Hinoel Zamis Ehrenbring ¹, Roberto Christ ^{2,*}, Fernanda Pacheco ¹, Leticia Wilhelms Francisco ¹, Giulia Cavagnoli Bolezina ¹, Natália Berwanger Hanauer ¹, Guilherme Gregio Grings ¹ and Bernardo Fonseca Tutikian ¹

¹ Polytechnical School, UNISINOS University, São Leopoldo 93040-230, Brazil; hzamis@unisininos.br (H.Z.E.); fepacheco@unisininos.br (F.P.); leticiawilhelms@gmail.com (L.W.F.); giulia.bolezina@edu.unisininos.br (G.C.B.); natalia_hanauer@hotmail.com (N.B.H.); grings.engenharia@outlook.com (G.G.G.); bftutikian@unisininos.br (B.F.T.)

² Department of Civil and Environmental, Universidad de la Costa, Barranquilla 080002, Colombia

* Correspondence: rchrist@cuc.edu.cu

Abstract: The materials used in civil construction are undergoing significant advances to achieve reduced maintenance and increased durability. This study analyzed the self-cleaning potential of Glass fiber Reinforced Concrete (GRC) with the addition of titanium dioxide (TiO₂) in contents of 3, 5, and 7% with respect to the mass of cement. We evaluated the self-cleaning GRC plates and the compressive and flexural strength of cylindrical and prismatic specimens. Prepared GRC sample plates were stained with dye solution (rhodamine B and methylene blue) and exposed to the four cardinal solar orientations of a building façade (north, south, east, and west) at different inclination angles (0°, 45°, and 90°) with respect to ground level. Results showed that the samples that presented the greatest performance were plates positioned in a north orientation and inclined at 0° in relation to ground level. The inclusion of TiO₂ positively affected the consistency of the mixtures and improved the properties of the GRC in the hardened state. Measured rupture stresses were greater than 100 MPa in compressive strength and 20 MPa in flexure. The results of this study showed that the introduction of TiO₂ in concrete with high strengths did have great relevance for the self-cleaning of white concrete.

Keywords: glass fiber reinforced concrete; self-cleaning concrete; titanium dioxide; maintenance of buildings



Citation: Ehrenbring, H.Z.; Christ, R.; Pacheco, F.; Francisco, L.W.; Bolezina, G.C.; Hanauer, N.B.; Grings, G.G.; Tutikian, B.F. Analysis of the Self-Cleaning Potential of Glass Fiber Reinforced Concrete (GRC) with TiO₂ Nanoparticles. *Sustainability* **2022**, *14*, 8738. <https://doi.org/10.3390/su14148738>

Academic Editor: Antonio Conforti

Received: 11 May 2022

Accepted: 8 June 2022

Published: 17 July 2022

Publisher's Note: MDPI stays neutral with regard to jurisdictional claims in published maps and institutional affiliations.



Copyright: © 2022 by the authors. Licensee MDPI, Basel, Switzerland. This article is an open access article distributed under the terms and conditions of the Creative Commons Attribution (CC BY) license (<https://creativecommons.org/licenses/by/4.0/>).

1. Introduction

White concrete and glass fiber reinforced concrete (GRC) have been used in building façade elements when aesthetics and sustainability characteristics are desired [1]. This result is achieved due to the reduction in coating materials (e.g., mortar and paint) applied to building façades and maintenance costs of this construction system [2]. Any façade elements are subjected to an elevated concentration of environmental pollution which dirties the surface and generates sustainability concerns [3].

GRC is a versatile and consolidated technology material that can be used in constructing façade elements. It has been used in façade elements since the early 1970's in more than 50 countries. It consists of a cement mixture reinforced with alkali-resistant fibers with high flexural strength [4,5]. This allows the manufacture of elements of reduced thickness and less specific weight [6]. When applied to façades, GRC allows standardization of the manufacture and assembly of panels which reduces costs with no decrease in performance. As such, GRC can be used in new buildings or in the restoration and rehabilitation of old ones [7].

GRC is considered a cementitious composite with ductile behavior which results in visible deformations and multiple cracking [8]. As reported by Iskender and Karasu [6], the fiber content in GRC improves its performance with respect to load absorption, impact resistance, and flexural and tensile strength. However, building façades are also often

subjected to staining due to weathering and urban pollution [9]. This process is not restricted to particles suspended in the atmosphere which accumulate on the surface but also includes the result of chemical reactions. These chemical reactions are induced by solar irradiation or inherent in the manufacture and assembly processes [10]. It was noted by Mansour and Al-Dawery [11] that the dirtying of a façade could be a result of the assembly and attachment technique used or the growth of microorganisms such as fungi and bacteria.

Façade preservation could be achieved with the application of products that decrease the accumulation of dirt or provide self-cleaning. A possible technique is the incorporation of titanium dioxide (TiO_2) in the cement matrix [11,12]. Titanium dioxide prevents the impregnation of dirt when exposed to solar irradiation [13]. Studies have shown that TiO_2 is a hydroxyl with photocatalytic and hygroscopic properties whose chemical reactions, when mixed in GRC, are accelerated under UV radiation [14]. Photocatalysis emulates natural photosynthesis adsorbed and contributes to the separation of electron pairs [15,16]. The activated photocatalyst promotes CO_2 photoreduction and contributes to the elimination of microorganisms [17,18].

Studies of self-cleaning TiO_2 -based products have confirmed that photocatalysis occurred under UV light. Treviso [19] tested mortar façades with 5%, 10%, and 15% of TiO_2 content and confirmed self-cleaning performance. Such mineral self-cleaning additives applied to façades and subjected to solar irradiation and water decreased the surface adhesiveness of particles, thus preventing the deposit of fine or organic materials even on rough surfaces. The speed of the self-cleaning oxidation reaction is related to UV intensity, temperature, relative humidity, TiO_2 content, and particle adhesiveness [11,18,20].

In cement matrices based on Portland Cement, TiO_2 is an inert material that does not participate in hydration reactions or react with any of the phases of cementitious composite. However, it has been determined by Ma et al. [21] to act as a filler that reduced pores and produced corresponding improvements in the compressive and flexural strength of the GRC. Sikora, Horszczaruk, and Rucinska [22] obtained similar improvements in these mechanical properties with a 3% TiO_2 content when compared to a reference sample. Application of TiO_2 could occur as a surface layer or incorporated into the concrete matrix. In this condition, it was confirmed as a filler material that reduced porosity but also reduced initial strength [7,14].

Additionally, if used in proportions of more than 1%, it negatively affected the workability of the concrete [19,20,23]. Stained samples subjected to UV radiation presented some color recovery, but this effect decreased over time and with higher proportions of TiO_2 .

Considering the presented scenario, it is possible to note a lack of studies evaluating the potential of self-cleaning GRC in authentic and natural exposure conditions and with different dirt elements. This study evaluates different percentages of TiO_2 in GRC samples containing glass fiber, considering the exposure in a roof slab with rhodamine B and methylene blue.

2. Materials and Methods

The experimental methodology consisted of tests on fresh and hardened GRC composite plates as well as visual analyses of the samples and spectrophotometry. The GRC composites incorporated increasing TiO_2 contents with respect to the mass of cement and were identified accordingly: GRC3 with 3%, GRC5 with 5%, and GRC7 with 7%.

Materials used for the manufacture of GRC were white Portland Cement type II, quartz sand, titanium dioxide, and AR glass fiber added as 0.5% with respect to total volume. The glass fibers used had a length of 10 mm and a diameter of 12 μm (shape factor of 833). The Polycarboxylate Ethers Superplasticizer (PCE-SP) was added at 1.5% with respect to cement. Table 1 presents the mix ratio, in mass, of the prepared samples.

Slump tests have been conducted in the past on fresh samples following the procedures of standard EN 1170-1 [24]. Mechanical properties were measured through compressive and flexural strength tests on a universal testing machine (INSTRON Machine testing). For the flexural tests, the ASTM C348:2021 [25] method was used. Six cylindrical specimens were

produced for each composite by age. That is, in total, 48 cylindrical tests were produced. For the prismatic samples, the same sampling was followed.

Table 1. Mix ratio of samples manufactured for this study (in mass).

Composite	Cement	Quartz Sand	TiO ₂ * %	Glass Fiber by % Volume **	w/c	SP * %
REF	1	1	0	0.5	0.2	1.5
GRC3	1	1	3	0.5	0.2	1.5
GRC5	1	1	5	0.5	0.2	1.5
GRC7	1	1	7	0.5	0.2	1.5

* addition proportion with respect to cement, ** proportion with respect to total volume of the mixture.

Color recoveries of the different TiO₂ contents were evaluated by saturating the plates with rhodamine B dye diluted in water in a solution of 0.5 g/L as recommended by Treviso [19]. Plates were immersed in the dye solution for 24h, followed by exposition to natural sunlight for 21 days followed by visual analyses. The procedure was repeated on the same plates with methylene blue in a 5.0 g/L solution as performed by Balbino [26], followed by exposition to natural sunlight for 21 days followed by spectrophotometry measurements. The plates were repurposed from the rhodamine B testing since façade elements are subjected to repeat dirtying. The color recovery testing procedure is shown in the flowchart in Figure 1.

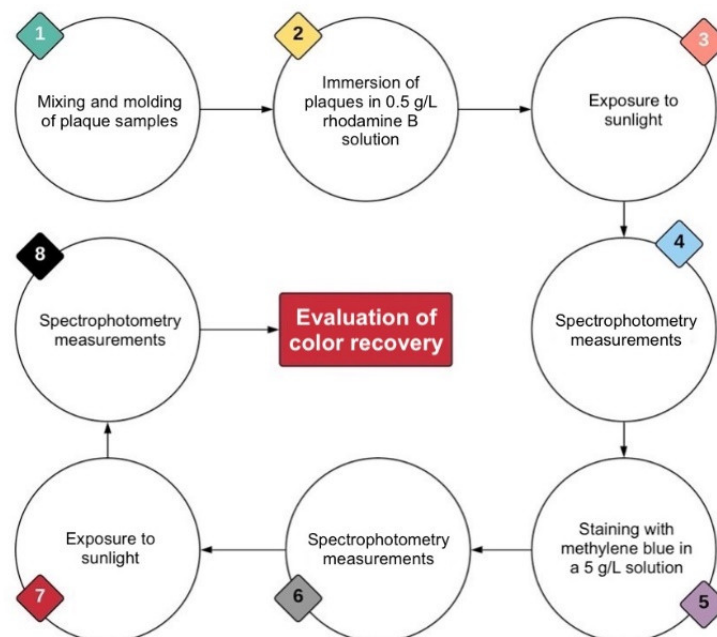


Figure 1. Flowchart of color recovery test.

Natural sunlight exposure was conducted in three distinct inclinations: 0°, 45°, and 90°. As shown in Figure 2, the plates were mounted on wooden frames which secured each inclination.

The frames were placed along the four cardinal orientations (north, south, east, and west) each inclination made use of four plates (coordinates: −29.79193720757752, −51.14931743845786) In total, 96 plates were used to analyze the self-cleaning capacity of the mixtures. Of these, 48 were stained with rhodamine B and 48 with methylene blue. The frames were mounted on the rooftop of an academic building at the Unisinos University campus as seen in Figure 3. The incident UV radiation was in the microclimate area of the city of São Leopoldo. This process was conducted for each type of dye for 21 days each.

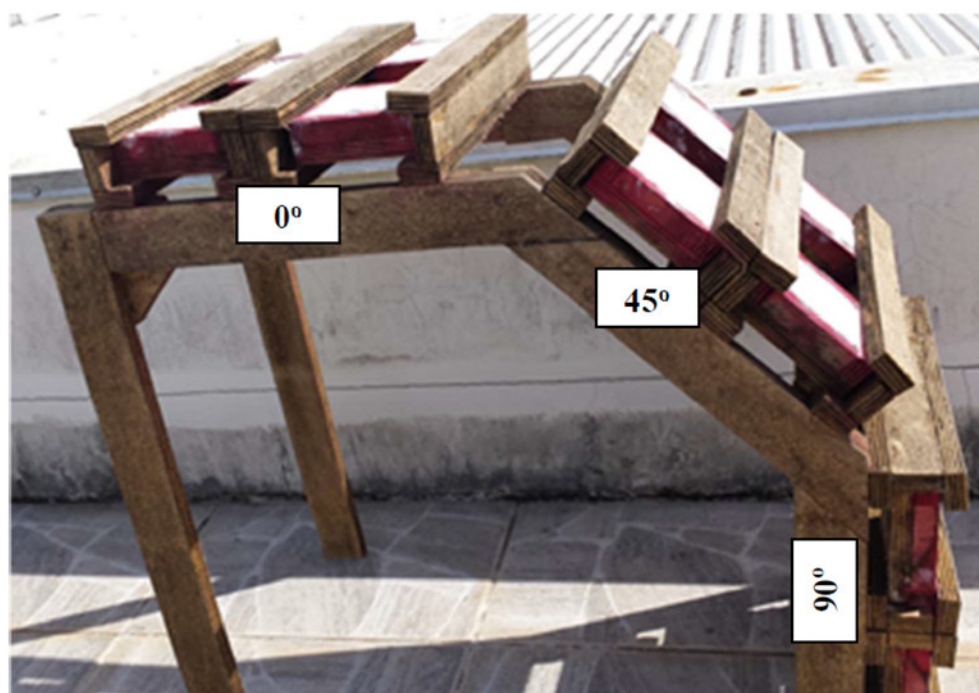


Figure 2. Wooden frame holding plates at distinct inclinations.



Figure 3. Geographical location of the color recovery test.

As reported by Santos [27], for a surface to receive the greatest radiation possible, it must be placed at the same inclination as the local latitude and at 0° (north) azimuth in the southern hemisphere as is the case of São Leopoldo. In addition to geographical considerations, Macphee and Folli [28] noted that TiO_2 activation was affected both by geographical and seasonal conditions. Since the exposure part of this study occurred between March and May, weather conditions during this period such as solar irradiation, precipitation, temperature, and relative humidity were also obtained. These variations are shown in Figure 4.

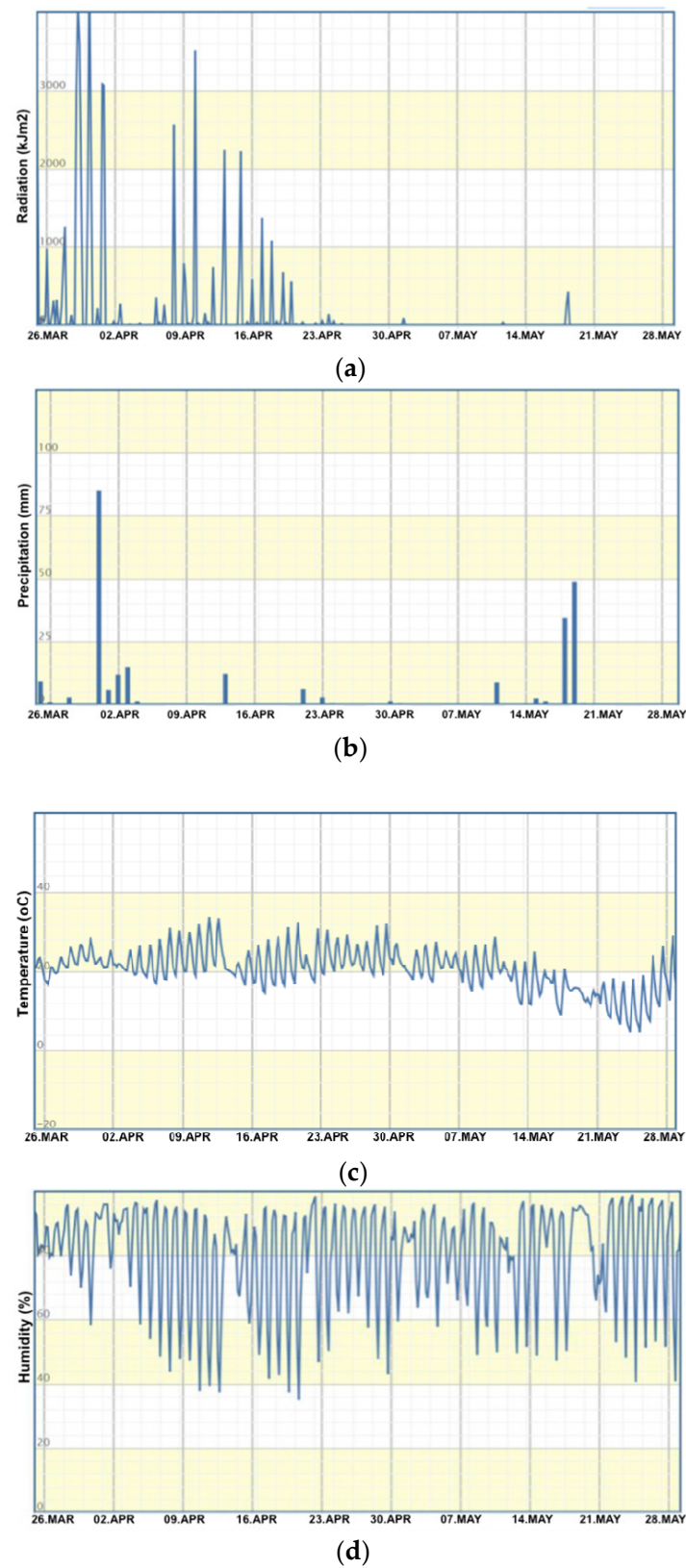


Figure 4. Weather conditions during the period of study. (a) Solar irradiation. (b) Precipitation. (c) Ambient temperature. (d) Relative humidity.

Spectrophotometry measures the light absorbed or transmitted through a solid medium. This equipment is used to measure the difference in the tone of the plates with specific

spectrophotometer coordinates denoted as L^* , a^* , and b^* . For example, a pure white color tone has reference coordinates $L^* = 100$, $a^* = 0$, and $b^* = 0$. As the surface becomes covered in dirt, the L^* coordinate decreases, and the a^* and b^* coordinates vary up or down depending on the tonality of the dirt (see Figure 5).

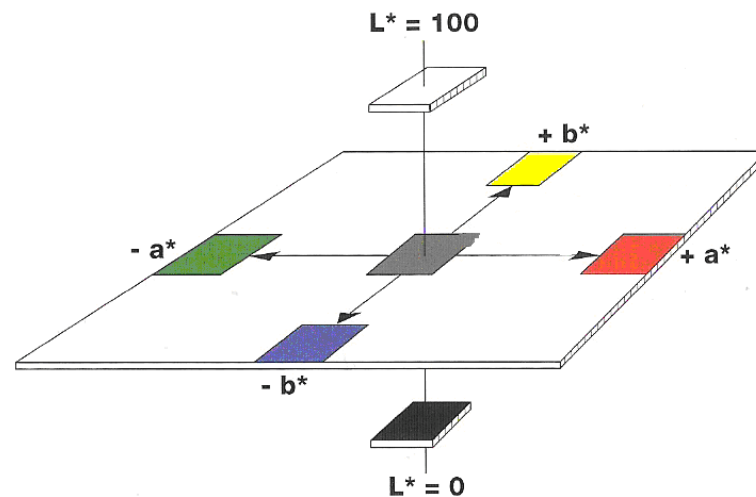


Figure 5. $L^*a^*b^*$ color space graph (CIELAB).

With the values of L^* , a^* , and b^* it is possible to calculate the color variation (ΔE), which is determined by Equation (1).

$$\Delta E = \sqrt{(\Delta L^2) + (\Delta a^2) + (\Delta b^2)} \quad (1)$$

For this study, these measurements accounted for TiO_2 content, orientation, and inclination of the plates. As TiO_2 activated and induced self-cleaning, spectrophotometer coordinates were expected to return to their initial values. It should be noted that the test plates of this study were not perfectly white and consequently had non-zero values for the initial a^* and b^* coordinate.

Readings were taken at 4 locations on each plate with a Konica Minolta portable spectrophotometer model CM-2500d. Readings were aided by a guide surface with cutouts 1 cm in diameter, with the equipment placed at the center of each cutout. Three sets of measurements were taken prior to the saturation with methylene blue (day 1), after saturation (day 2), and after 21 days of exposure to natural sunlight (day 3).

For self-cleaning and color recovery tests under ambient sunlight, plates measuring 120 mm \times 120 mm \times 20 mm (width \times length \times thickness) were produced with a single layer of each mixture into molds. This layer was mechanically densified using a vibration table. From the results, the dirtiness reduction index (ΔS) of each GRC was calculated, using Equation (2).

$$\Delta S(\%) = \left(\frac{\Delta E_{\text{inicial}} - \Delta E_{j,\text{days}}}{\Delta E_{\text{inicial}}} \right) \cdot 100 \quad (2)$$

Folli [29] noted that TiO_2 is inert. It did not react chemically with the other components of the cementitious matrix to increase strength but could contribute to filler effects. Figure 6 shows the granulometric curve of the materials in the mixture. As seen in the figure, TiO_2 had the smallest diameters among the other materials and, as such, was also designated as nano-titanium dioxide.

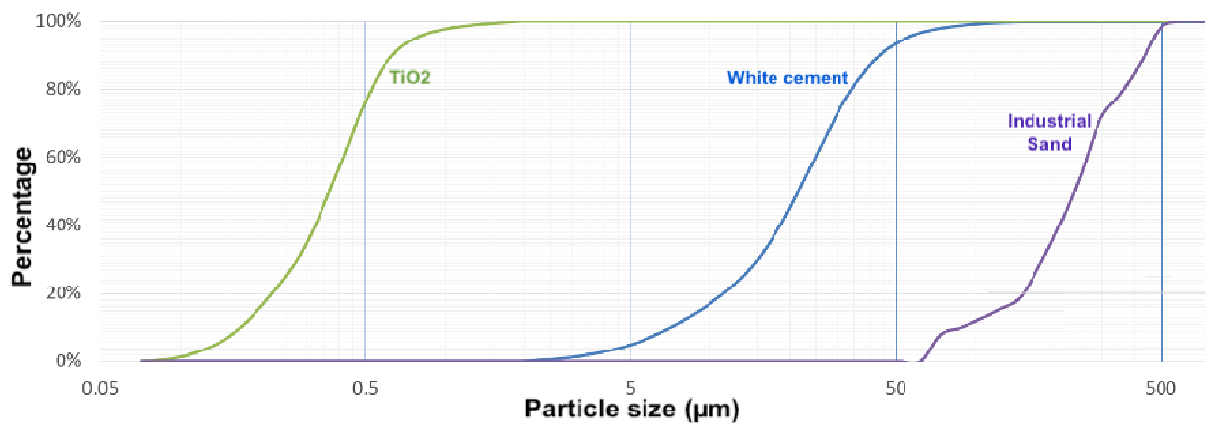


Figure 6. Granulometric curves of the materials in the mortar.

3. Results

3.1. Properties in the Fresh State

Slump test results are shown in Table 2. Table 2 displays a noticeable effect of TiO_2 : the slump diameter increases on average 10 mm proportionally to content.

Table 2. Slump test results.

Composite	Ø (mm)	Image	Composite	Ø (mm)	Image
REF	65		GRC5	90	
GRC3	75		GRC7	95	

The studies of Meng et al. [30] and Sorathiya et al. [31] reported that TiO_2 addition was proportionally detrimental to the fluidity of the cementitious matrix with increasing content. Decreased workability was also noted and attributed to the increase in specific surface area due to the presence of nano- TiO_2 [32]. Other studies such as Zapata et al. [33] and Mukharjee et al. [34] confirmed that the change in the characteristic of the concrete was related to the fineness modulus and surface area of TiO_2 particles. Reduced workability was also measured by Jalal et al. [35] as decreases in slump diameter of 10, 20, 40, 60, and 70 mm for TiO_2 contents of 1, 2, 3, 4, and 5%, respectively, in the mass of the mixture.

On the other hand, other studies have obtained results opposite to the previous trends. Noorvand et al. [36] evaluated the effect of TiO_2 added to black rice husk mortar. Results showed increased fluidity proportional to TiO_2 content with 30% rice husk substitution. This effect was believed to be associated with the filler effect of TiO_2 in the pores of the matrix. Mohseni et al. [37] also demonstrated improved workability with higher TiO_2 content and the slump diameter was increased by as much as 5.3% with respect to a

reference mixture. This result was attributed to the sphericity of TiO₂ particles. This behavior may also have occurred in this study, increasing the fine content and thus, with filler effect.

3.2. Compressive and Flexural Strength Results

Average strengths and standard deviation of axial compressive and flexural strength tests of the mixtures at 7 days and 28 days of curing are shown in Table 3.

Table 3. Compressive and flexural strength results.

Composite	Compressive Strength (MPa)		Flexural Strength (MPa)	
	7 Days	28 Days	7 Days	28 Days
REF	93.1 ± 5.0	118.1 ± 3.0	17.9 ± 3.0	19.7 ± 3.0
GRC3	99.5 ± 1.1	118.3 ± 2.6	20.2 ± 4.0	20.8 ± 4.0
GRC5	105.2 ± 6.0	120.0 ± 3.0	18.2 ± 1.0	20.3 ± 1.0
GRC7	96.3 ± 7.0	121.8 ± 2.0	17.8 ± 3.0	21.4 ± 2.0

At 7 days, the compressive strength increased with increasing TiO₂ content up to 5%, which matched the results of Linsebigler et al. [38]. At this age, GRC5% obtained the highest compressive strength among the composites and the difference between them was up to 13%. This positive effect from small additions of TiO₂ was also observed in Ma et al. [21]. Although it did not follow a linear increasing trend, sample GRC7 still presented a higher compressive strength than the reference, as with all the other samples. A similar trend is observed at 28 days of curing but with the overall values closer to the reference sample strength. Still, in this case, sample GRC7 presented the highest compressive strength.

An understanding of the effects of TiO₂ on compressive strength could be gained by examining grain packing in the concrete mixtures. Yunsheng et al. [39] reported that increased strength and decreased porosity could be traced to the packing particle curve since finer particles increased density by reducing void spaces. This effect would be assisted by the inert nature of TiO₂, which did not react with any of the concrete phases or take part in cement hydration reactions.

Table 3 shows that TiO₂ did not induce substantial gains in flexural strength. Overall, results followed Fernandes [40] and Austria [41], who determined that a 10% TiO₂ content yielded the most increase in flexural strength, albeit a small one. Austria [41] noted that this is possibly a consequence of the fineness of the material resulting in a filler effect. Fiber reinforcement was known to improve matrix post-cracking performance due to the reduced spacing between reinforcement elements when compared to a conventional material [42,43].

3.3. Plate Color (before Staining)

Differences in surface tonality were observed immediately after demolding the plates. As shown in Figure 7, samples were gradually lighter in tone as TiO₂ content increased.

This was expected since TiO₂ is considered a pigment and used as a whitening and opacity agent in other products such as coatings, plastics, paints, glasses, and others [44] and this effect was known to be proportional to TiO₂ concentration. This way, the staining of the plates with titanium dioxide was more apparent in the larger plates due to the difference in the white tone. However, evaluations related to the staining reduction index were carried out among the specimens of each sample in different periods.

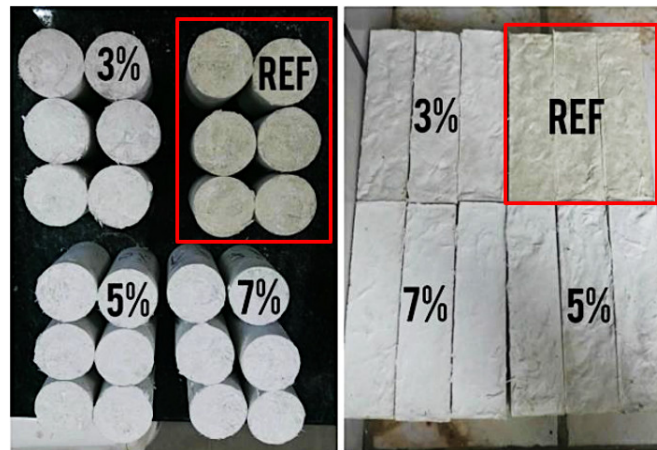


Figure 7. Visual appearance of some samples immediately after demolding: cylinders (left) and prismatic (right).

3.4. Visual Analysis with Rhodamine B

This chapter will present the results obtained with plates impregnated with rhodamine B. As mentioned in the introduction section, the UV incidence reacts with TiO_2 allowing the plates to self-clean, and thus, the angulation and orientation play an important role in the mentioned effect.

Figure 8 presents visual results of plate samples impregnated with rhodamine B with respect to preset inclinations of 0° , 45° , and 90° and a north orientation.

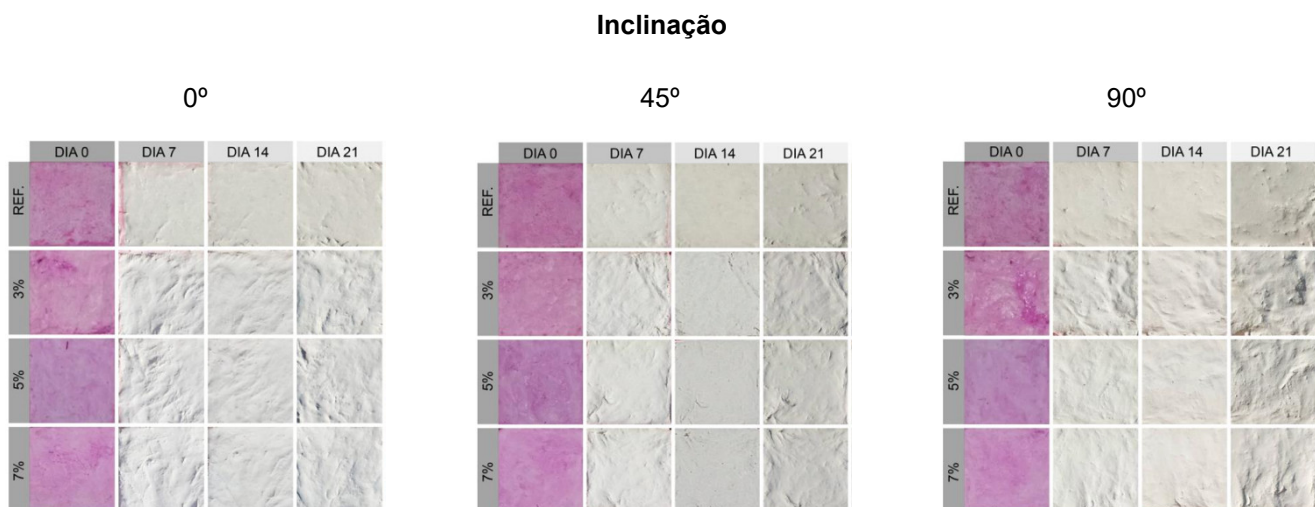


Figure 8. Visual dirtiness of plates stained with rhodamine B facing north.

As seen in Figure 8, sample GRC7 obtained the best results with lighter tonality in all inclinations. It should be noted that most rhodamine B staining was removed after 7 days and the remaining staining along the edges disappeared after 14 days. The north orientation resulted in the most UV incidence and, coupled with precipitation between day 7 and day 21, induced sufficient rhodamine B decomposition chemical reactions. This result partially matched Treviso [19], which obtained the most change in color with a north orientation and 45° inclination, with 0° and 90° not too far behind. In the case of this study, an inclination of 0° yielded the best lighter color results at 14 days and at 21 days. This was likely a result of water accumulation due to the horizontal inclination of the plate. In contrast, Burger and R  ther [45] concluded that, at high latitudes, a vertical position (as in 90°) was the most favorable for solar irradiation. As for cleaning time, Sikora et al. [22] claimed that TiO_2 cleaning effects could be triggered in as short as two hours of exposition.

Figure 9 presents visual results of the plates with respect to preset inclinations of 0° , 45° , and 90° and an east orientation.

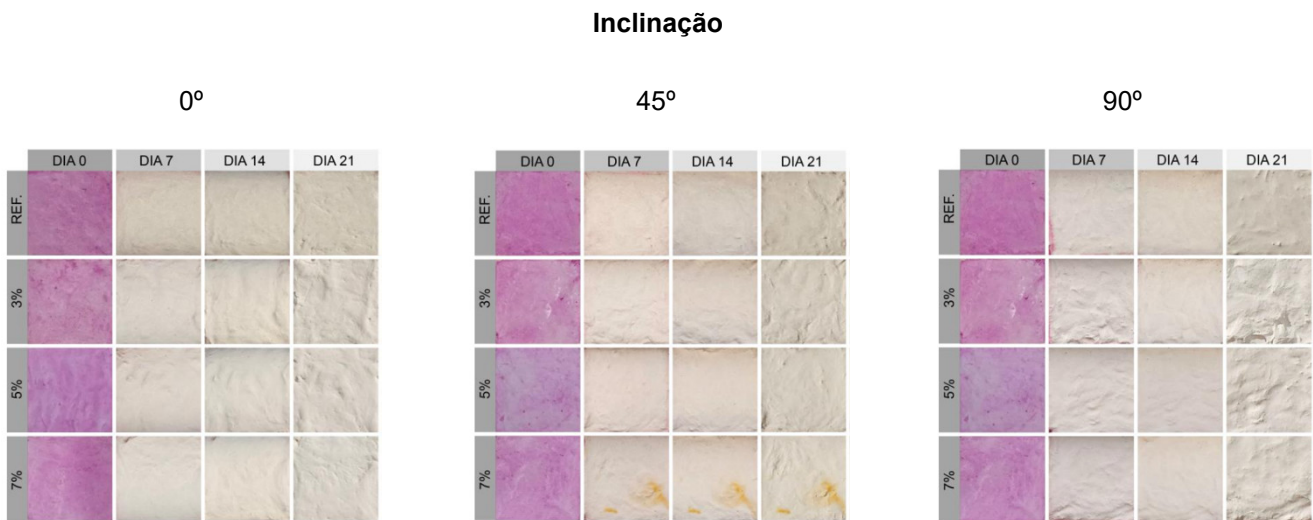


Figure 9. Visual dirtiness of plates stained with rhodamine B facing east.

Results of Figure 9 show that east-oriented plates did not present the same self-cleaning evolution as the north orientation of Figure 8. The reference and sample GRC3 inclined at 0° and 90° still displayed traces of color at 14 days. The same traces could be observed for sample GRC5 at a 45° inclination. Sample GRC7 inclined at 45° showed staining due to the oxidation of the molds immersed in rhodamine B, which was not removed by the self-cleaning process since it was not organic in nature. This was previously verified by Diamanti et al. [46] in that inorganic iron oxide reduced the self-cleaning ability of GRC. Beeldens [47] also noted that TiO_2 was only able to degrade organic dirtying and not iron oxide staining. Figure 9 also demonstrates that there was little visible difference between inclinations of 0° and 90° although the plates at 0° still presented some advantage probably due to deformations caused by the accumulation of water.

Figure 10 presents visual results of the plates with respect to preset inclinations of 0° , 45° , and 90° and a west orientation.

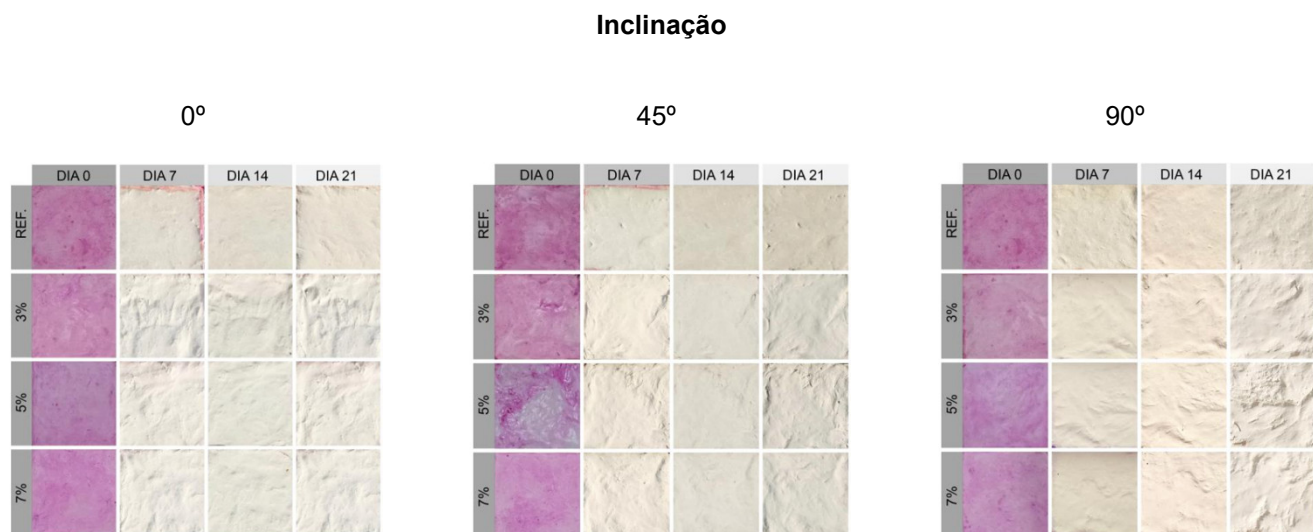


Figure 10. Visual dirtiness of plates stained with rhodamine B facing west.

Figure 10 shows that, for all preset inclinations, results were similar for all samples but GRC7 presented the best performance. Overall, most staining had degraded by day 7

with some coloration remaining along the edges of the reference sample, which did not last past day 14. For a west orientation, it should be noted that the best result was obtained at 0° . Considerable apparent deformations were observed at 90° , probably due to water accumulation on the rough surface which was unable to runoff due to the inclination.

Figure 11 presents visual results of the plates with respect to preset inclinations of 0° , 45° , and 90° and a south orientation.

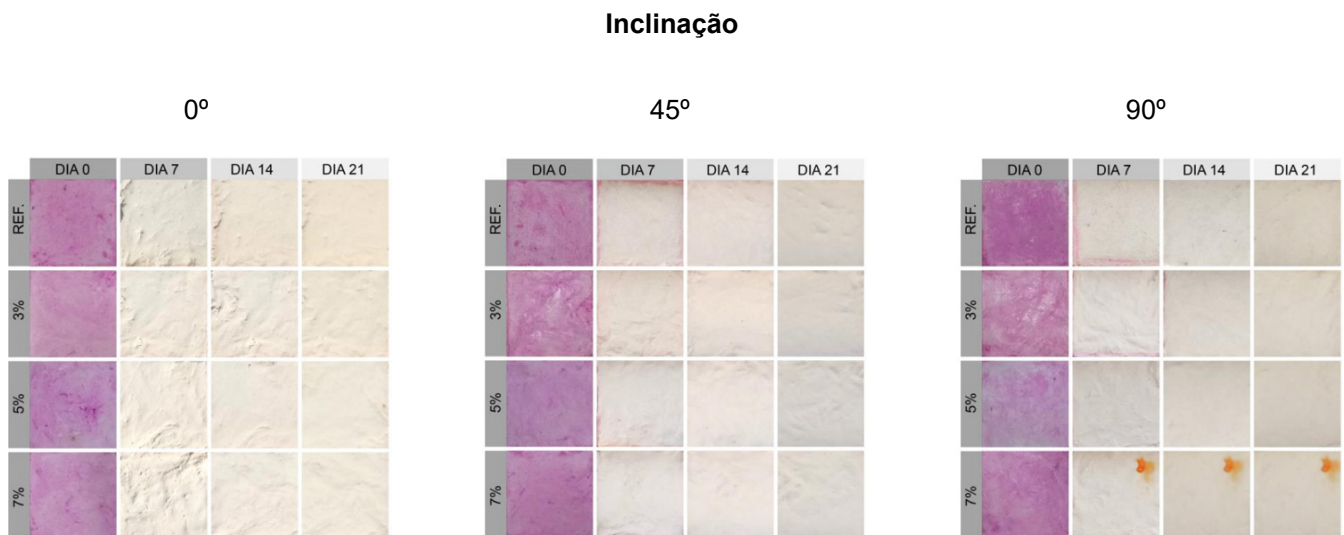


Figure 11. Visual dirtiness of plates stained with rhodamine B facing south.

Figure 11 shows that sample GRC7 at 0° inclination presented the best result with all staining degraded by day 7. On the other hand, GRC7 plates with a 90° inclination presented inorganic oxidation stains which were not degraded as expected. Overall, the south-facing plates presented the most difference between inclinations compared with the other orientations with 0° being lighter and 90° more stained.

3.5. Visual and Spectrophotometric Analysis of Methylene Blue Staining

The GRC plates stained with methylene blue were also exposed to 21 days of natural sunlight. Throughout this period, no precipitation occurred from day 0 to day 7 but was present between day 7 and day 21. Consequently, the reductions in dirtiness presented in the first 7 days of exposure were the consequence of UV radiation only. Results are presented in Figure 12 for plate inclinations of 0° , 45° , and 90° .

Results of Figure 12 show that the dirtiness reduction index (ΔS) was nearly identical for all GRC samples in the first 7 days of exposure. This was not only observed across all GRC samples but also regardless of orientation or inclination. It should be stressed that no precipitation occurred during this period and thus stressed the role of water as a trigger for TiO_2 reactions. Diamanti et al. [46] pointed out that water was a necessary component in TiO_2 -based self-cleaning compounds since it contributed to the activation and release of chemical substances that decreased the dirtiness of surfaces.

In addition to the absence of water, the low ΔS index observed in the first 7 days was also a result of the effect of the contaminant on the surface of the plates, which reduced the amount of UV radiation passing through to the GRC matrix. The layer of dirt and contaminants on the sample's surface may have hampered for UV rays to penetrate until they reached the TiO_2 contained in the GRC. Since TiO_2 was effectively blocked from the UV rays, chemical reactions were retarded and so was the self-cleaning effect. Despite the lack of water and blocked UV rays, the GRC matrices with TiO_2 addition still presented a higher ΔS than the reference sample. Past day 7, dirtiness decreased both visually and on the ΔS index curve from precipitation and degradation of the contaminant layer, which

progressively allowed more UV rays to penetrate the matrix. These external parameters were also cited by Diamanti et al. [46] as relevant to the effectiveness of self-cleaning.

Overall, increases in TiO₂ content in the cementitious matrix resulted in greater reductions in staining. Consequently, sample GRC7 with 7% TiO₂ addition presented the most promising results with an ΔS of up to 93%. The effects of concentration became more evident depending on UV exposure conditions. Thus, a 0° inclination coupled with a north or west orientation had the most intense and longest UV exposure, which resulted in more active TiO₂ reactions and a self-cleaning effect as reported by Treviso [19].

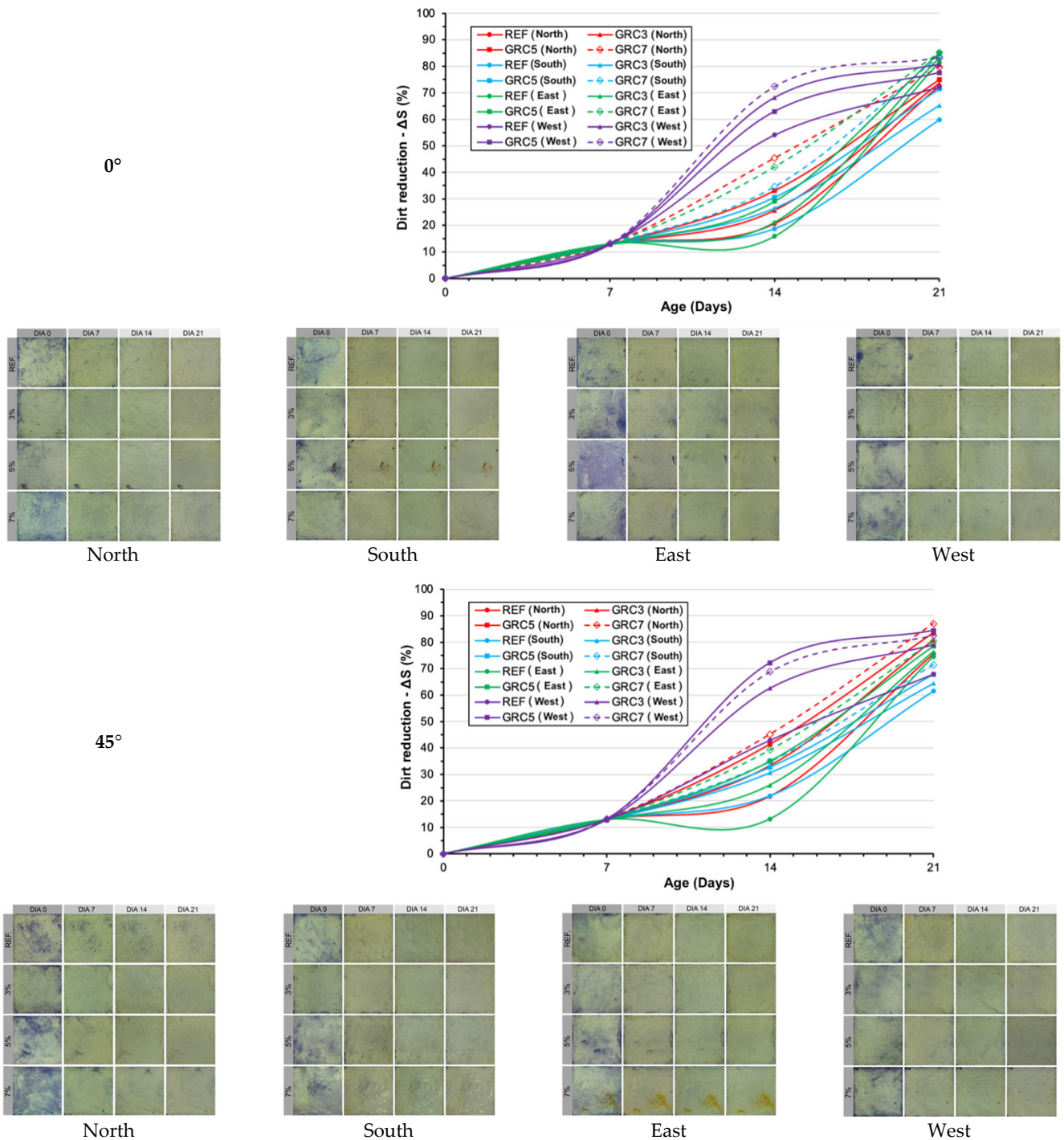


Figure 12. Cont.

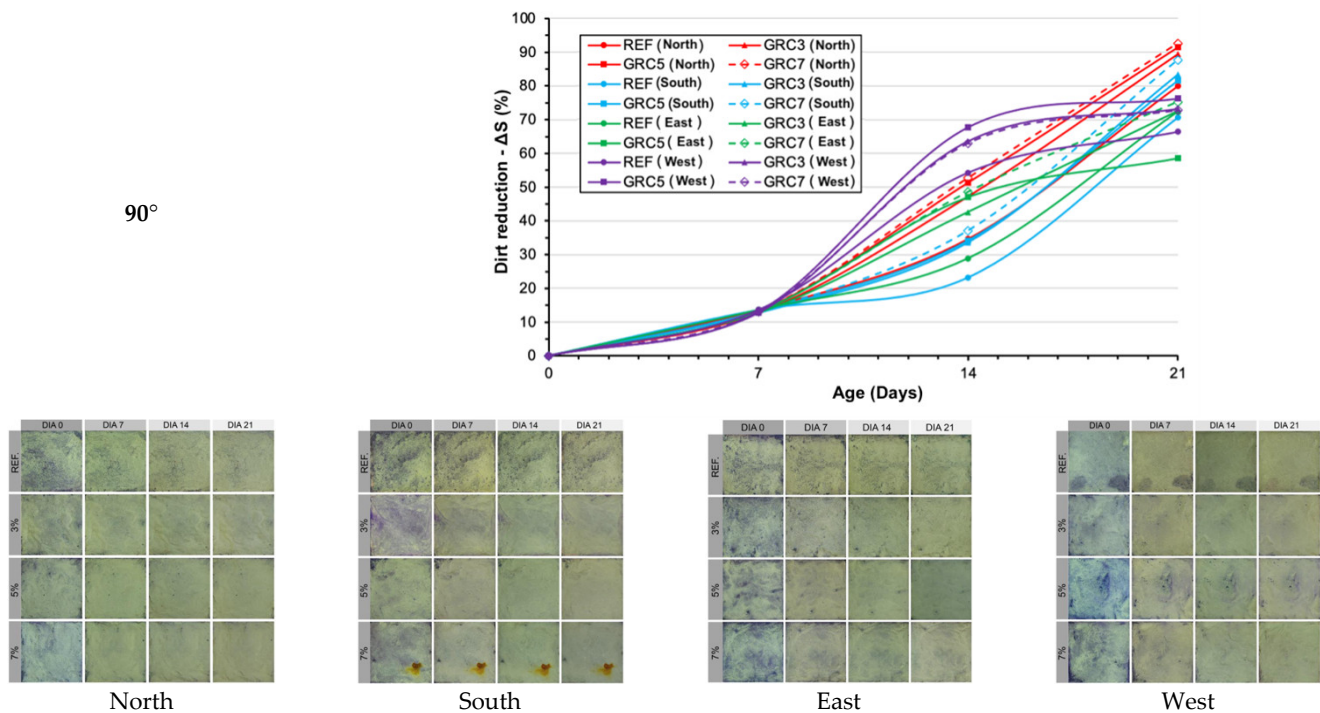


Figure 12. Visual results and dirtiness reduction index (ΔS) curve for plates stained with methylene blue at cardinal directions and inclinations of 0° , 45° , and 90° .

The reference sample also presented reductions in staining, but these were related to degradation from natural cycles of wetting and drying. In this process, dirtiness indices (ΔS) were over 50% especially in plates with a north orientation. However, there was visible residual staining which was much more noticeable than in the plates with TiO_2 content.

Evaluating the effect of inclination, fewer ΔS indices corresponded to 90° . At this inclination, UV incidence was unfavorable, and, at certain periods of the day, shades were observed on the surface of the plates. For the plates at 90° and with a south orientation, ΔS varied from 57% to 93% which demonstrated the severe impact of shading on the effectiveness of the self-cleaning action of TiO_2 .

Surface temperature also played a role as significant as the presence of water and UV incidence. Plate temperature can intensify TiO_2 chemical reactions and accelerate the self-cleaning effect. In theory, that would result in decreased performance in plates facing south and east since those should have lower temperatures. In practice, results showed little variation in ΔS between south and east-facing samples regardless of TiO_2 content. However, plates with the same inclination and facing north presented increasing differences in ΔS as TiO_2 content increased, with GRC7 samples having the best performance.

4. Conclusions

This study evaluated the effect of TiO_2 addition on the self-cleaning and compressive and flexural strength of the GRC plates. Sample GRC7, with 7% of TiO_2 in the mass of cement reached a higher dirtiness reduction index (ΔS) after 21 days of exposition. In relation to ΔS , it was already expected that the results would be better than the other mixtures due to the physicochemical functioning of the compound. The following conclusions were drawn from this study:

Higher TiO_2 content resulted in higher self-cleaning as there were visible improvements in self-cleaning effects when compared to the reference sample. Due to the location of São Leopoldo in the Southern hemisphere, the best results were obtained with the plates facing north. While variations in inclination were not as effective, a horizontal 0° inclination had the best result from the incidence of solar irradiation throughout the day.

TiO₂ did not produce a self-cleaning effect on inorganic materials during the relatively short term of this study. Further, long-term studies should be performed to confirm this phenomenon.

The layer of dirt and contaminants on the surface of the samples may have made it difficult for UV rays to penetrate until they reached the TiO₂ contained in the GRC, resulting in variations in the self-cleaning results. Thus, depending on the contaminant and exposure conditions to which the plates are exposed, self-cleaning is not guaranteed only by increasing the concentration of TiO₂.

The solar orientation directly influenced the ΔS results of the samples, since it is related to the exposure to UV rays and the time of insolation. However, the inclination of the plates was also decisive, since the best results were obtained at 45°. On this slope, good levels of insolation and the presence of water/moisture on the face after exposure to rain were observed. Water was an important precursor agent for TiO₂ activation, in addition to favoring the runoff of dirt through “washing”.

Author Contributions: L.W.F., G.C.B., G.G.G. and N.B.H., development of the experimental tests and results compilation. H.Z.E., F.P. and R.C., results analysis, discussion, and comparisons with research sources. B.F.T., review of results and valuable contributions in their interpretation. All authors have read and agreed to the published version of the manuscript.

Funding: This research received no external funding.

Institutional Review Board Statement: Not applicable.

Informed Consent Statement: We declare consent.

Data Availability Statement: We declare data availability.

Acknowledgments: The authors are grateful for the assistance received in carrying out the tests and purchasing raw materials, especially from Itt Performance—UNISINOS.

Conflicts of Interest: We declare that there is no conflict of interest.

References

1. Chira, A.; Kumar, A.; Vlach, T.; Laiblová, L.; Hajek, P. Textile-reinforced concrete facade panels with rigid foam core prisms. *J. Sandw. Struct. Mater.* **2016**, *18*, 200–214. [[CrossRef](#)]
2. Sayed, N.; Afify, M. The Evolution of green cladding technology for architectural façades and its role in achieving environmental integration. *J. Environ. Treat. Tech.* **2001**, *9*, 548–558.
3. García, L.D.; Pastor, J.M.; Peña, J. Self-cleaning and depolluting glass reinforced concrete panels: Fabrication, optimization and durability evaluation. *Constr. Build. Mater.* **2018**, *162*, 9–19. [[CrossRef](#)]
4. Cuypers, H.; Wastiels, J.; Van Itterbeeck, P.; De Bolster, E.; Orłowski, J.; Raupach, M. Durability of glass fibre reinforced composites experimental methods and results. *Compos. Part A Appl. Sci. Manuf.* **2006**, *37*, 207–215. [[CrossRef](#)]
5. Cuypers, H.; Wastiels, J. Analysis and verification of the performance of sandwich panels with textile reinforced concrete faces. *J. Sandw. Struct. Mater.* **2011**, *13*, 589–603. [[CrossRef](#)]
6. Iskender, M.; Karasu, B. Glass fiber reinforced concrete pipes. *Nat. Water Council Bull.* **2018**, *5*, 136–162.
7. Ortolan, V.K.; Francisco, L.W.; Cadore, B.C.; Ott, M.J.; Christ, R. Análise da influência geométrica de fibra de vidro AR na matriz cimentícia de GRC. In Proceedings of the 59° Congresso Brasileiro do Concreto, Bento Gonçalves, Brazil, 31 October–3 November 2017; pp. 1–11.
8. Pacheco, F.; Toma, N.; Ortolan, V.; Marques, M.; Ehrenbring, H.; Montelongo, A.; Christ, R.; Tutikian, B. Residual life identification of an industrial building through non-destructive tests and mathematical models of damage. In Proceedings of the 9th International Conference on Concrete under Severe Conditions—Environment & Loading, Porto Alegre, Brazil, 5–7 June 2019. [[CrossRef](#)]
9. Silva, A.; De Brito, J.; Gaspar, P.L. *Methodologies for Service Life Prediction of Buildings: With a Focus on Façade Claddings*; Springer: Berlin/Heidelberg, Germany, 2016.
10. Wittmann Lanzarin, B.; Folle, L.F. Análise da estética do concreto produzido com rejeito plástico para o uso no design de interiores com viés sustentável. *MIX Sustentável* **2020**, *6*, 61–72. [[CrossRef](#)]
11. Mansour, A.M.H.; Al-Dawery, S.K. Sustainable self-cleaning treatments for architectural facades in developing countries. *Alex. Eng. J.* **2018**, *57*, 867–873. [[CrossRef](#)]
12. Maggonage, R.E.F.A. Performance of NO₂ Sequestered Recycled Concrete Aggregate (NRCA) incorporated Ordinary Portland Cement (Opc) Concrete. Ph.D. Thesis, Clarkson University, Potsdam, NY, USA, 2020.

13. Díaz-Hernández, D.Z.; Sarmiento-Alipio, J.A. Concreto a Base de Cenizas Volantes Activadas Alcalinamente, Modificado con Nanopartículas de Óxido de Silicio y Dióxido de Titanio. Master's Thesis, Universidad Católica De Colombia, Bogotá, Colombia, 2020.
14. Nosrati, R.; Olad, A.; Najjari, H. Study of the effect of TiO₂/polyaniline nanocomposite on the self-cleaning property of polyacrylic latex coating. *Surf. Coat. Technol.* **2017**, *316*, 199–209. [[CrossRef](#)]
15. González, E.; Bonnefond, A.; Barrado, M.; Barrasa, A.M.C.; Asua, J.M.; Leiza, J.R. Photoactive self-cleaning polymer coatings by TiO₂ nanoparticle Pickering miniemulsion polymerization. *Chem. Eng. J.* **2015**, *281*, 209–217. [[CrossRef](#)]
16. Low, J.; Cheng, B.; Yu, J. Surface modification and enhanced photocatalytic CO₂ reduction performance of TiO₂: A review. *Appl. Surf. Sci.* **2017**, *392*, 658–686. [[CrossRef](#)]
17. Nikokavoura, A.; Trapalis, C. Alternative photocatalysts to TiO₂ for the photocatalytic reduction of CO₂. *Appl. Surf. Sci.* **2017**, *391*, 149–174. [[CrossRef](#)]
18. Tan, L.-L.; Ong, W.-J.; Chai, S.-P.; Mohamed, A.R. Photocatalytic reduction of CO₂ with H₂O over graphene oxide-supported oxygen-rich TiO₂ hybrid photocatalyst under visible light irradiation: Process and kinetic studies. *Chem. Eng. J.* **2017**, *308*, 248–255. [[CrossRef](#)]
19. Treviso, J.P.M. Avaliação da Eficiência de Autolimpeza em Argamassas e Pastas Contendo TiO₂ Expostas ao Microclima Urbano. Master's Thesis, Universidade Federal do Rio Grande do Sul, Porto Alegre, Brazil, 2016.
20. Masheane, M.; Nthunya, L.; Mubiayi, M.; Thamae, T.; Mhlanga, S. Physico-chemical characteristics of some Lesotho's clays and their assessment for suitability in ceramics production. *Part. Sci. Technol.* **2018**, *36*, 117–122. [[CrossRef](#)]
21. Ma, B.; Li, H.; Mei, J.; Li, X.; Chen, F. Effects of nano-TiO₂ on the toughness and durability of cement-based material. *Adv. Mater. Sci. Eng.* **2015**, *2015*, 583106. [[CrossRef](#)]
22. Sikora, P.; Horszczaruk, E.; Rucinska, T. The effect of nanosilica and titanium dioxide on the mechanical and self-cleaning properties of waste-glass cement mortar. *Procedia Eng.* **2015**, *108*, 146–153. [[CrossRef](#)]
23. Moro, C.; El Fil, H.; Francisco, V.; Velay-Lizancos, M. Influence of water-to-binder ratio on the optimum percentage of nano-TiO₂ addition in terms of compressive strength of mortars: A laboratory and virtual experimental study based on ANN model. *Constr. Build. Mater.* **2021**, *267*, 120960. [[CrossRef](#)]
24. BS EN 1170-1:1998; Precast Concrete Products. Test Method for Glass-Fiber Reinforced Cement. Measuring the Consistency of the Matrix. 'Slump Test' Method. European Standards: Pilsen, Czech Republic, 1998.
25. ASTM C348:2021; Standard Test Method for Flexural Strength of Hydraulic-Cement Mortars. ASTM International (ASTM): West Conshohocken, PA, USA, 2021.
26. Balbino, R.O. Remoção do Corante Azul de Metileno por Fotocatálise Heterogênea com Radiação UV Artificial e Dióxido de Titânio (TiO₂) como Catalisador. Bachelor's Thesis, Universidade Tecnológica Federal do Paraná (UTFPR), Campo Mourão, Brazil, 2015.
27. Santos, I.P. Minicurso building-integrated photovoltaics para arquitetos e engenheiros civis. In Proceedings of the V Congresso Brasileiro de Energia Solar, Sao Paulo, Brazil, 11–12 March 2014.
28. Macphee, D.; Folli, A. Photocatalytic concretes—The interface between photocatalysis and cement chemistry. In Proceedings of the Materials Research Society Meeting (ISCM), João Pessoa, Brazil, 28 September–2 October 2014.
29. Folli, A. TiO₂ Photocatalysis in Portland Cement Systems: Fundamentals of Self-Cleaning Effect and Air Pollution Mitigation. Ph.D. Thesis, University of Aberdeen, Aberdeen, Scotland, 2010.
30. Meng, T.; Yu, Y.; Qian, X.; Zhan, S.; Qian, K. Effect of nano-TiO₂ on the mechanical properties of cement mortar. *Constr. Build. Mater.* **2012**, *29*, 241–245. [[CrossRef](#)]
31. Sorathiya, J.; Shah, S.; Kacha, S. Effect on addition of nano "titanium dioxide" (TiO₂) on compressive strength of cementitious concrete. *Kalpa Publ. Civ. Eng.* **2017**, *1*, 219–225. [[CrossRef](#)]
32. Khitab, A.; Anwar, W. *Advanced Research on Nanotechnology for Civil Engineering Applications*; Mirpur University of Science and Technology: New Mirpur City, Pakistan, 2016.
33. Zapata, L.E.; Portela, G.; Suárez, O.M.; Carrasquillo, O. Rheological performance and compressive strength of superplasticized cementitious mixtures with micro/nano-SiO₂ additions. *Constr. Build. Mater.* **2013**, *41*, 708–716. [[CrossRef](#)]
34. Mukharjee, B.B.; Barai, S.V. Influence of nano-silica on the properties of recycled aggregate concrete. *Constr. Build. Mater.* **2014**, *55*, 29–37. [[CrossRef](#)]
35. Jalal, M.; Fathi, M.; Farzad, M. Effects of fly ash and TiO₂ nanoparticles on rheological, mechanical, microstructural and thermal properties of high strength self-compacting concrete. *Mech. Mater.* **2013**, *61*, 11–27. [[CrossRef](#)]
36. Noorvand, H.; Ali, A.A.A.; Demirboga, R.; Farzadnia, N.; Noorvand, H. Incorporation of nano TiO₂ in black rice husk ash mortars. *Constr. Build. Mater.* **2013**, *47*, 1350–1361. [[CrossRef](#)]
37. Mohseni, E.; Miyandehi, B.M.; Yang, J.; Yazdi, M.A. Single and combined effects of nano-SiO₂, nano-Al₂O₃ and nano-TiO₂ on The mechanical, rheological and durability properties of self-compacting mortar containing fly ash. *Constr. Build. Mater.* **2015**, *84*, 331–340. [[CrossRef](#)]
38. Linsebigler, A.L.; Lu, G.; Yates, J.T. Photocatalysis on TiO₂ surfaces: Principles, mechanisms, and selected results. *Chem. Rev.* **1995**, *95*, 735–758. [[CrossRef](#)]
39. Yunsheng, Z.; Wei, S.; Sifeng, L.; Chujie, J.; Jianzhong, L. Preparation of C200 green reactive powder concrete and its static–dynamic behaviors. *Cem. Concr. Compos.* **2008**, *30*, 831–838. [[CrossRef](#)]

40. Fernandes, C. Estudo Sobre Incorporação de Nanopartículas de Dióxido de Titânio em Argamassas Fotocatalíticas. Ph.D. Thesis, Universidade Federal do Ceará, Fortaleza, Brazil, 2017.
41. Austria, G.C. Argamassa Autolimpante para Revestimentos de Fachadas: O Efeito das Propriedades Fotocatalíticas do Dióxido de Titânio (TiO₂). Master's Thesis, UFRGS, Porto Alegre, Brazil, 2015.
42. Quinino, U.C.M. Investigação Experimental das Propriedades Mecânicas de Compósitos de Concreto Com Adições Híbridas de Fibras. Ph.D. Thesis, Universidade Federal do Rio Grande do Sul, Porto Alegre, Brazil, 2015.
43. De Souza, R.P.; Pacheco, F.; Prager, G.L.; Gil, A.M.; Christ, R.; de Mello, V.M.; Tutikian, B.F. Verification of the influence of loading and mortar coating thickness on resistance to high temperatures due to fire on load-bearing masonries with clay tiles. *Materials* **2019**, *12*, 3669. [[CrossRef](#)]
44. Gázquez, M.J.; Bolívar, J.P.; Tenorio, F.G.; Vaca, F. A review of the production cycle of titanium dioxide pigment. *Mater. Sci. Appl.* **2014**, *5*, 441–458. [[CrossRef](#)]
45. Burger, B.; Ruther, R. Inverter sizing of grid-connected photovoltaic systems in the light of local solar resource distribution characteristics and temperature. *Sol. Energy* **2006**, *80*, 32–45. [[CrossRef](#)]
46. Diamanti, M.V.; Del Curto, B.; Ormellese, M.; Pedferri, M.P. Photocatalytic and self-cleaning activity of colored mortars containing TiO₂. *Mater. Chem. Eng.* **2013**, *46*, 167–174. [[CrossRef](#)]
47. Beeldens, A. *An Environmental Friendly Solution for Air Purification and Self-Cleaning Effect: The Application of TiO₂ as Photocatalyst in Concrete*; Belgian Road Research Centre: Brussels, Belgium, 2006.